A Conservative CIP Method for Violent Free Surface Flows

Changhong Hu and Masashi Kashiwagi
Research Institute for Applied Mechanics, Kyushu University, Fukuoka, Japan
hu@riam.kyushu-u.ac.jp

1 Introduction

In the past several years, continuous effort has been made in RIAM, Kyushu University to develop an efficient Cartesian grid method for violent free surface problems in ship and ocean engineering. Our researches have been focused on

(1) Accurate and robust flow solver for multi-phase flows with solid bodies.
(2) Conservative and smearingless interface capturing scheme.

In the numerical method, violent wave-body interaction is treated as multi-phase problem and solved numerically in a Cartesian grid. The CIP (Constrained Interpolation Profile) algorithm [1] was adopted as the base scheme for the flow solver. It has been proved by a number of numerical examples that the CIP method is accurate and robust enough for such multi-phase problems [2][3][4]. For capturing the immersed boundaries (free surfaces), we have improved and applied the CIP-CSL3 scheme [3] and THINC scheme [4] to our CFD code and their efficiency was investigated. Both schemes are conservative and smearingless.

In this research we consider to improve the conservation property of flow solver since the CIP scheme we are using for advection calculation is not a conservative one. In some marine applications, e.g., simulation of violent tank sloshing in which long physical time phenomena and free surface impact phenomena are need to consider, conservation property of the CFD code, both for the flow solver and the interface capturing method, is an important factor that affects the computation quality. In a violent tank sloshing experiment [3], we have measured the pressure on the sidewall. For some cases two pressure peaks in one oscillation period were observed while in the computation the second peak could not be properly predicted. We considered that the use of non-conservative CIP scheme may cause it because some of the momentum of fluid might be lost during the impact of the fluid onto the wall in the computation.

As the framework of our CIP based CFD code works well so far, in the current development we retain all the features of the code except for the flow solver in which the CIP scheme is replaced by the CIP-CSL2 (Constrained Interpolation Profile – Conservative Semi-Lagrangian scheme with 2nd order polynomial function) scheme [5]. The mathematical formulation and numerical details are described in this paper and some preliminary validation cases are presented.

2 Numerical Method

The details of our CIP/Cartesian grid method can be found in the papers [2][4]. Here we only describe the CIP-CSL2 scheme and the new flow solver based on it.

2.1 Conservative CIP Scheme

We consider 1-D advection equation for ϕ as:

$$\frac{\partial \phi}{\partial t} + \frac{\partial u\phi}{\partial x} = 0 \tag{1}$$

By integration of Eq. (1) over a computation cell $[x_{i-1/2}, x_{i+1/2}]$ we have

$$\frac{\partial \bar{\phi}_i}{\partial t} = -\frac{1}{\Delta x_i}\left[(u\phi)_{i+1/2} - (u\phi)_{i-1/2}\right] \tag{2}$$

where $\overline{\overline{\phi}}_i = \frac{1}{\Delta x_i}\int_{x_{i-1/2}}^{x_{i+1/2}} \phi(x,t)\,dx$ is the cell volume averaged value and $(u\phi)_{i\pm1/2}$ is the numerical flux at the cell boundary. They can be computed by a Semi-Lagrangian method using the following 2nd order interpolation function.

$$\Psi_i(x) = c_0 + c_1(x - x_{i-1/2}) + c_2(x - x_{i-1/2})^2 \qquad (3)$$

In CIP-CSL2 scheme, we define volume integrated averaging (VIA) $\overline{\overline{\phi}}_i$ and surface integrated averaging (SIA) or point value (PV) for 1-D case $\phi_{i\pm1/2}$ in one cell as shown in Fig. 1. They are used for determining the interpolation function (3).

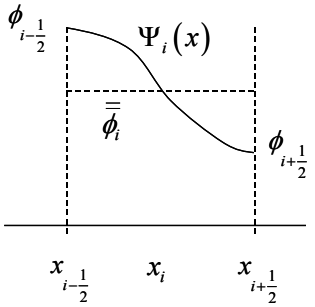

Fig.1 1-D Computation cell for CIP-CSL2

The three unknown parameters in (3), c_0, c_1 and c_2, are obtained by using the following conditions.

$$\Psi_i(x_{i-1/2}) = \phi_{i-1/2}, \quad \Psi_i(x_{i+1/2}) = \phi_{i+1/2},$$
$$\frac{1}{\Delta x_i}\int_{x_{i-1/2}}^{x_{i+1/2}} \Psi_i(x)\,dx = \overline{\overline{\phi}}_i \qquad (4)$$

2.2 Flow Solver

. The governing equations for an unsteady viscous, incompressible fluid written in general conservation lows are

$$\int_S \mathbf{u}\cdot\mathbf{n}\,dS = 0 \qquad (5)$$

$$\frac{\partial}{\partial t}\int_V \mathbf{u}\,dV + \int_S \mathbf{u}(\mathbf{u}\cdot\mathbf{n})\,dS = -\int_S \frac{p}{\rho}\mathbf{n}\,dS + \frac{1}{\rho}\int_S \mathbf{T}_{ij}\cdot\mathbf{n}\,dS + \int_V \mathbf{f}\,dV \qquad (6)$$

where V and S stand for volume and surface of a control volume, respectively. $\mathbf{T}_{ij}$ is the viscous stress tensor. The last term on the right hand side (RHS) of Eq. (6) is due to the body force, such as the gravity force, etc. The coupling of velocity and pressure can be made by the projection method, in which the pressure is solved by the following Poisson equation.

$$\int_S \nabla\left(\frac{p^{n+1}}{\rho}\right)\cdot\mathbf{n}\,dS = -\int_S (\mathbf{u}^{**}\cdot\mathbf{n})\,dS \qquad (7)$$

For a three dimensional computation, if we consider a computation cell (i, j, k) as the control volume, definition of the VIA and SIA for all quantities is shown in Fig. 2. The VIA of velocity is denoted by $\overline{\overline{u}}_\alpha$, which is defined at the cell center as well as the pressure and the density. Here $\alpha = 1, 2, 3$. The SIAs of velocity are denoted by ${}^x\overline{u}_\alpha$, ${}^y\overline{u}_\alpha$ and ${}^z\overline{u}_\alpha$, which are defined at the cell surface center. A full set of VIA and SIA discretization formulation of the governing equations is called VSIAM3 (Volume/Surface Integrated Average based Multi-Moment Method) [7]. In this study we propose a simplified treatment. Instead of solving separated equations for VIA and SIA of (6), we solve only one of them and using the following linear interpolation to update the other.

$$\left.\begin{aligned} d^{x}\overline{u}_{\alpha\,i,j,k} &= \frac{1}{2}\left(d\overline{\overline{u}}_{\alpha\,i,j,k} + d\overline{\overline{u}}_{\alpha\,i-1,j,k}\right) \\ d^{y}\overline{u}_{\alpha\,i,j,k} &= \frac{1}{2}\left(d\overline{\overline{u}}_{\alpha\,i,j,k} + d\overline{\overline{u}}_{\alpha\,i,j-1,k}\right) \\ d^{z}\overline{u}_{\alpha\,i,j,k} &= \frac{1}{2}\left(d\overline{\overline{u}}_{\alpha\,i,j,k} + d\overline{\overline{u}}_{\alpha\,i,j,k-1}\right) \end{aligned}\right\} \qquad (8)$$

$$\left.\begin{aligned} d\overline{\overline{u}}_{\alpha\,i,j,k} &= \frac{1}{2}\left(d^{x}\overline{u}_{\alpha\,i,j,k} + d^{x}\overline{u}_{\alpha\,i+1,j,k}\right) \\ d\overline{\overline{u}}_{\alpha\,i,j,k} &= \frac{1}{2}\left(d^{y}\overline{u}_{\alpha\,i,j,k} + d^{y}\overline{u}_{\alpha\,i,j+1,k}\right) \\ d\overline{\overline{u}}_{\alpha\,i,j,k} &= \frac{1}{2}\left(d^{z}\overline{u}_{\alpha\,i,j,k} + d^{z}\overline{u}_{\alpha\,i,j,k+1}\right) \end{aligned}\right\} \qquad (9)$$

By applying a fractional step approach, the time evolution of Eq. (6) can be divided into three calculation steps: one advection step and two no-advection steps. The advection calculation is carried by CIP-CSL2 in the present

flow solver.

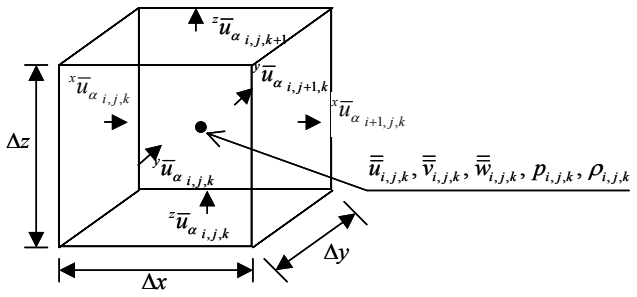

Fig. 3 Definition of VIA and SIA of velocities in a computation cell.

Advection step

We start each time step calculation with the advection step from the known velocity field $\overline{\overline{u}}_\alpha^n$, ${}^x\overline{u}_\alpha^n$, ${}^y\overline{u}_\alpha^n$ and ${}^z\overline{u}_\alpha^n$.

At the advection step, only the left hand side (LHS) of (6) is considered.

$$\frac{\partial}{\partial t}\int_V \mathbf{u}dV + \int_S \mathbf{u}\left(\mathbf{u}\cdot\mathbf{n}\right)dS = 0 \tag{10}$$

To solve the multi-dimensional equation (10) by the one-dimensional CIP-CSL2 scheme that is described in *Section 2.1*, a directional splitting technique is used. Let $\left(u_A, v_A, w_A\right)$ be the advection velocity, we conduct the following procedure.

(i) Calculation in *x*-direction.

$$\frac{\partial u_\alpha}{\partial t} + \frac{\partial u_A u_\alpha}{\partial x} = 0 \tag{11}$$

We obtain ${}^x\overline{u}_\alpha^{*1}$ and $\overline{\overline{u}}_\alpha^{*1}$ by CIP-CSL2, and use (8) to have ${}^y\overline{u}_\alpha^{*1}$ and ${}^z\overline{u}_\alpha^{*1}$.

(ii) Calculation in *y*-direction.

$$\frac{\partial u_\alpha}{\partial t} + \frac{\partial v_A u_\alpha}{\partial y} = 0 \tag{12}$$

We obtain ${}^y\overline{u}_\alpha^{*2}$ and $\overline{\overline{u}}_\alpha^{*2}$ by CIP-CSL2, and use (8) to have ${}^x\overline{u}_\alpha^{*2}$ and ${}^z\overline{u}_\alpha^{*2}$.

(iii) Calculation in *z*-direction.

$$\frac{\partial u_\alpha}{\partial t} + \frac{\partial w_A u_\alpha}{\partial z} = 0 \tag{13}$$

We obtain ${}^z\overline{u}_\alpha^{*}$ and $\overline{\overline{u}}_\alpha^{*}$ by CIP-CSL2, and use (8) to have ${}^x\overline{u}_\alpha^{*}$ and ${}^y\overline{u}_\alpha^{*}$. These are the first intermediate values after advection step calculation.

Non-advection step (i)

In this step, all terms in RHS of (6) except for those related to pressure are solved by the following equation.

$$\frac{\overline{\overline{u}}_i^{**} - \overline{\overline{u}}_i^{*}}{\Delta t} = \frac{1}{V_{ijk}\rho}\int_S \mathbf{T}_{ij}^{*}\cdot\mathbf{n}dS + \overline{\overline{f}}_i \tag{14}$$

where $V_{ijk} = \Delta x_i \Delta y_j \Delta z_k$. We obtain the second intermediate values $\overline{\overline{u}}_i^{**}$ and then ${}^\beta\overline{u}_i^{**}$ by (8).

Non-advection step (ii)

In this step we treat the velocity-pressure coupling. The Poisson equation (7) is rewritten here using the VIA quantities:

$$\frac{\partial}{\partial x_i}\left(\frac{1}{\rho}\frac{\partial p^{n+1}}{\partial x_i}\right) = -\frac{1}{\Delta t}\left(\frac{\partial {}^x\overline{u}^{**}}{\partial x} + \frac{\partial {}^y\overline{v}^{**}}{\partial y} + \frac{\partial {}^z\overline{w}^{**}}{\partial z}\right) \tag{15}$$

Solution of this equation gives the pressure field for the new time level.

The velocities at cell surface for the new time step can be obtained as follows.

$$\frac{{}^\alpha\overline{u}_\alpha^{n+1} - {}^\alpha\overline{u}_\alpha^{**}}{\Delta t} = -\frac{1}{\rho}\frac{\partial p^{n+1}}{\partial x_\alpha} \tag{16}$$

Finally, $\overline{\overline{u}}_i^{n+1}$ is obtained by (9).

2.3 Treatment of Immersed Solid Bodies

In this new method, solid bodies are treated by FAVOR technique [7], in which open volume fraction and open area fraction are used. The efficiency of the treatment is demonstrated by a 2-D simulation of uniform flow past a circular cylinder.

3 Numerical Results

3.1 Flow past a circular cylinder

2-D computation on a uniform flow past a circular cylinder is carried out with the proposed

numerical method. The Reynolds number is 200 and a uniform mesh with the grid point number of 300×150 and grid spacing of $D/20$ is used. Here D is the diameter of the cylinder. As shown in Fig.4, computed velocity vectors near the body surface are reasonable. The computed mean drag force, lift force amplitude and Strouhal number are 1.27, 0.35 and 0.21, respectively, which compare well to the experiment.

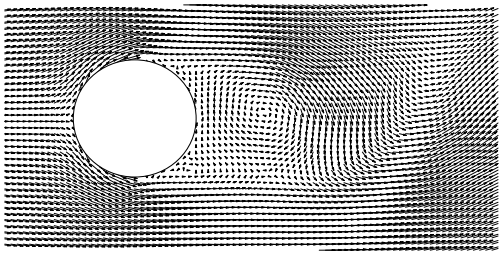

Fig.4 Uniform flow past a circular cylinder at Re=200

3.2 Violent sloshing in a rectangular tank

This example is taken from an experimental problem [3]. The schematic view of the experiment is shown in Fig. 5. The filling height is h=12cm. The motion of the tank is $y = A\sin(2\pi/T)$, with A=5cm and T=1.40sec. Three pressure gauges, p_1, p_2 and p_3 are installed at the right vertical wall.

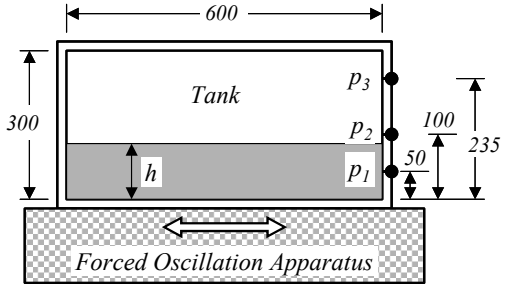

Fig.5 Schematic view of tank sloshing experiment

In the present 3D computation a uniform grid is used, with the grid point number of $200\times100\times40$. The computations are carried out using two different flow solvers, one denoted by 'Conservative CIP' that is proposed in this paper and the other by 'original CIP' that has been used up to now.

In Fig. 6, comparisons among the two computations and the experiment of pressure time series at P_2 are shown. This is the two-peak pressure profile case in the experiment. The original CIP flow solver failed to predict the second peak. The new conservative CIP method, however, gives a fairly good prediction of this second peak.

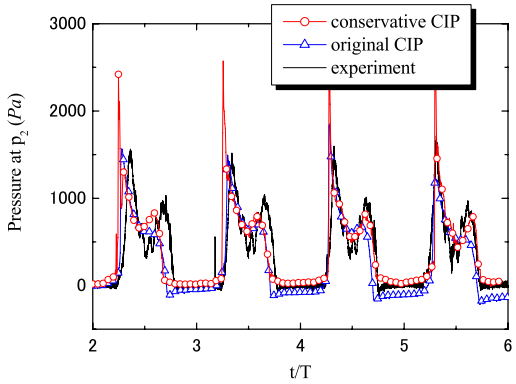

Fig.6 Comparison of pressure at P_2

References

[1] Yabe, T., Xiao, F. and Utsumi, T. (2001) The Constrained Interpolation Profile Method for Multiphase Analysis, J. Comput. Phys., 169: 556-593

[2] Hu, C. and Kashiwagi, M. (2004) A CIP-Based Method for Numerical Simulations of Violent Free Surface Flows, J. Marine Science and Technology, 9: 143-157

[3] Kishev, Z., Hu, C. and Kashiwagi, M. (2006), Numerical simulation of violent sloshing by a CIP-based method J. Marine Science and Technology, Vol. 11, pp. 111-122

[4] Hu, C. and Kashiwagi, M. (2007). Numerical and Experimental Studies on Three-Dimensional Water on Deck with a Modified Wigley Model, Proc. 9th Int. Conf. on Numerical Ship Hydrodynamics, Michigan, USA, V1, 159-169.

[5] Xiao, F. and Yabe, T. (2001) Completely conservative and oscillation-less semi-Lagrangian schemes for advection transportation, J. Comput. Phys., 170: 498-522

[6] Xiao, F., Ikebata, A. and Hasegawa, T. Numerical simulations of free interface fluids by a multi-integrated moment method, Computers and Structures 83 (2005) 409-423

[7] Hirt C.W., Volume –fraction techniques: powerful tool for wind engineering. J Wind Eng Ind Aerodyn 1993, 46-47: 327-38